NUMERICAL SIMULATIONS OF AN ACTIVE REGION STARTING WITH A REAL MAGNETOGRAM AS INITIAL CONDITIONS

CRISTIANA DUMITRACHE

Astronomical Institute of Romanian Academy
Str. Cutitul de Argint 5, 40557 Bucharest, Romania
Email: crisd@aira.astro.ro

Abstract. We numerically investigated the eruptive processes in an active region, starting with real observational data as initial values for the magnetic field. These data imply non-linear initial value and the very difficult conditions for the numerical simulations, often leading to numerical instabilities. To avoid the numerical instabilities, we have used a 2D code with a low resolution numerical grid. The numerical experiments have implied three steps, three procedures: (a) obtaining the coronal magnetic field by extrapolating it from the measured photospheric one, and to be used as initial values to the MHD simulations; (b) numerical MHD simulations, in order to obtain the magnetic field and plasma characteristics evolutions; (c) we have added computations of the force-free field parameter, representing the torsion and magnetic helicity estimation in the active region. Our results faithfully reproduce the astronomical observations.

Key words: solar physics – magnetic fields – active regions – helicity – coronal magnetic field extrapolations – MHD numerical simulations.

1. INTRODUCTION

The active regions are characteristic features of the solar activity. They represent the largest concentration of the magnetic flux and emerge from the solar interior as compact bipolar regions. They appear from the under photospheric zones and extend into the solar atmosphere inside all the layers (photosphere, chromosphere, and corona). They have a long lifetime and evolve during months and they are place of the main activity of the star. During their evolution they develop many explosive events, as flares in the chromosphere and coronal mass ejections (CMEs) in corona. During the big flares, the coronal mass ejections appear and manifest in the corona and leave the star influencing so the interplanetary medium and planets.

Observations have shown that the photospheric magnetic field is organized in discrete flux tubes embedded in near force-free plasma (Fan *et al.*, 1993). As Stenflo (1989) explained, we can distinguish between two categories of close magnetic field lines topology: one derives from the active regions and the other from the X-ray bright points zones (and having short lifetime, under 12 hours.) A magnetogram is organized as a distribution of footpoints of the magnetic field lines anchored in the photosphere and under it (Stenflo, 1989). Using other Sun's observations like

soft X-ray or EUV images, we deduce the topology of the magnetic field lines in the solar atmosphere as being close magnetic field organized in loops or open magnetic field lines extending into the interplanetary space. The solar magnetic field can be directly measured only in photosphere, and, recently, in the chromosphere (*e.g. Hinode* spacecraft), but never in the corona. The coronal magnetic field is inferred by extrapolation computations from the photospheric magnetograms (MDI/SOHO or HMI/SDO spacecraft's instruments), using various models.

Our interest for the explosive events affecting the Earth or the interplanetary space implies the investigation of the coronal magnetic field, the dynamics of the magnetic loops and their reconnections. How evolves a magnetohydrodynamic system in the case of a quit stage of the active region and what happen in the explosive events case? Does the initial magnetogram contain itself the potential for flares and CMEs?

Many of the MHD numerical codes deal with the coronal magnetic field. They integrate the MHD equations' system starting with an initial configuration and boundary conditions. The MHD approximations rely on the plasma behaving like a fluid in the magnetic field - we consider here plasma as a single fluid. The purpose of our non-linear force free fields numerical experiments is to investigate the magnetic field and plasma parameters evolution in an active region, starting with a real magnetogram as initial data for the magnetic field topology, and to compare the results with the observational data. These numerical investigations should start with a initial configuration of the coronal magnetic field, consequently, before the MHD simulations an algorithm to obtain the coronal field from the photospheric one must be considered. In section 2 we discuss the numerical methods applied in our experiments. Section 3 describes a particular observational case of an active region that we choose in our study (NOAA09845). The helicity evolution of the active region, as computed from the magnetic field extrapolations, is described in section 4. In section 5 we display the results of the numerical experiments performed at different moments, in the vicinity of a flare's time and CME occurrence in the active region. The last section contains the discussions and lessons we learned in these numerical experiments.

2. THE COMPUTATIONAL METHODS

The computational method implies two main steps: (A) preparation of the data and (B) the MHD numerical simulations.

(A) First stage of the numerical experiment requires the data preparation. We started with a MDI magnetogram and obtained the 3D coronal magnetic field components, $\overrightarrow{B} = (Bx, By, Bz)$, by an non-linear force-free field code. The 3D coronal magnetic field extrapolation was performed using an IDL code written by Lee (2002);

Lee and Gary (2003)).

A magnetic field dipole is defined by

$$\begin{aligned} Bx &= B0 \cdot \frac{3xz}{r^5} \\ By &= B0 \cdot \frac{3yz}{r^5} \\ Bz &= -B0 \frac{(1-3 \cdot \frac{z^2}{r^2})}{r^3} \end{aligned}$$

where $r = \sqrt{x^2+y^2+z^2}$ and $B0$ scales the strength of the magnetic field. The IDL code detects the positions of few pairs of magnetic dipoles, associated with the coronal image, in Cartesian coordinates and on the MDI magnetograms, by choosing the local extremes for each polarity. Finding the locations of the dipoles from the magnetogram involves two steps: finding the *xy* coordinates of the major or dominate dipoles and than finding the z coordinates.

(B) For the MHD numerical simulations we used a Flux Corrector Transport type 2D Fortran code, based on SHASTA (sharp and smooth transport algorithm). This code was developed by Weber (1978) and previously by Boris and Book (1973). Detailed descriptions of the code were made by Forbes and Priest (1982), and more recently by Dumitrache (1999).

The MHD equations are integrated by this code, named *Alfven Code*, on a mesh 49×97 points.

$$\frac{\partial \rho}{\partial t} + \overrightarrow{\nabla}(\rho \cdot \overrightarrow{v}) = 0 \tag{1}$$

$$\rho[\frac{\partial \overrightarrow{v}}{\partial t} + (\overrightarrow{v} \cdot \overrightarrow{\nabla})\overrightarrow{v}] = -\overrightarrow{\nabla}(p) + (\overrightarrow{B} \cdot \overrightarrow{\nabla}) \cdot \overrightarrow{B} - \overrightarrow{\nabla} \cdot (\frac{B^2}{2}) + \rho \cdot \overrightarrow{g} \tag{2}$$

$$\frac{\partial \overrightarrow{B}}{\partial t} = \overrightarrow{\nabla} \times (\overrightarrow{v} \times \overrightarrow{B}) + \eta \overrightarrow{\nabla}^2 \cdot \overrightarrow{B} \tag{3}$$

$$\frac{\rho^\gamma}{\gamma - 1} \frac{d}{dt}(\frac{p}{\rho^\gamma}) = -\overrightarrow{\nabla}(k \overrightarrow{\nabla} T) - \rho^2 Q(T) + j^2/\sigma + h\rho \tag{4}$$

$$p = \rho T \tag{5}$$

The initial configuration requires $v_x = 0$, $v_z = 0$, $\rho = 1$ and the following boundary conditions:

at top (x=1): $\frac{\partial B_z}{\partial x} = \frac{\partial B_z}{\partial x} = 0$; $\frac{\partial B_z}{\partial x} = -\frac{\partial B_x}{\partial z}$;

at right (z=1): $\frac{\partial B_x}{\partial z} = \frac{\partial B_z}{\partial z} = 0; \frac{\partial B_z}{\partial z} = -\frac{\partial B_x}{\partial x};$

at left - the symmetry axis: (z=0) $\frac{\partial B_x}{\partial z} = B_z = 0;$

at bottom (x=0): $\frac{\partial B_x}{\partial x} = \frac{\partial B_z}{\partial x} = 0.$

The initial magnetic field configuration is $\overrightarrow{B} = (Bx, Bz)$, where Bx and Bz are the coronal magnetic field, and the OX direction is oriented on the vertical axis. We have performed simulations in the XOZ plane of the 3D Cartesian coordinates system, using the extrapolated data as initial values of the magnetic field, using a 2D MHD code based on SHASTA method Weber (1978). An important attention has to be payed to the coordinate axis since OZ becomes OX, and OX becomes OZ, in the second step of computations.

3. THE OBSERVATIONAL DATA FOR THE ACTIVE REGION NOAA09845

The active region NOAA09845 (or simply noted AR9845) was registered on the solar disk between 23 February 2002 and 7 March 2002. Located on the Sun at N17 latitude and W18 longitude, on 2 March 2002, this active region was classified as Hale class $\beta\gamma\delta/\beta\gamma\delta$ and as McIntosh class Eki/Eai. The figure (1) displays the magnetogram of the active region at 20:04:00 UT, on 2 March 2002, *i.e.* the moment we choose to start the numerical simulations.

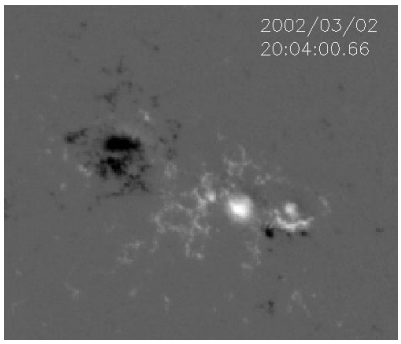

Fig. 1 – The MDI/SOHO image of AR9845, at 20:04:00 UT, on 2 March 2002.

More flares occurred in this day in AR9845, but only one, registered on 2 March 2002, gave a CME. Before this flare-CME onset, bright loops oscillating were revealed by EIT observations. The CME was orientated toward Ulysses aircraft position, which crossed over the solar pole at that time (Dumitrache *et al.*, 2010). We focuss now on the 2 March 2002 flare, occurred when this active region changed its polarity from beta to beta-gamma. A Hα associated flare, C4.4 type, was

registered at 20:10 UT (NOAA, Space Environment Center, cited by `http://www.solarmonitor.org/`). An interesting phenomenon observable on EIT/SOHO images happened before the flare occurrence, namely oscillations of the coronal loops in the active region, few hours before the flare start. The flare evolution as seen in the $H\alpha$ line is displayed the figure 2. We remark a recrudescence of the flare at 20:13 UT, mentioned in the NOAA catalogue as sub-flare class (SF).

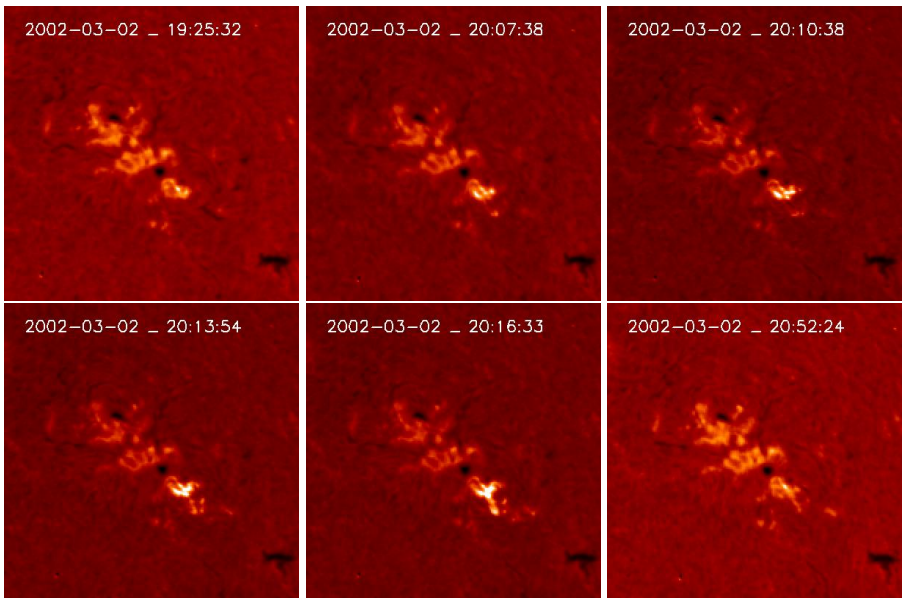

Fig. 2 – The Hα images of the C4.4 flare occurred in AR9845.

4. THE HELICITY EVOLUTION

A reasonable measure of the helicity in an active region is given by the torsion factor α estimation. The force-free parameter α of the magnetic field is computed by

$$\alpha = \frac{1}{Bz} \cdot \left(\frac{\partial By}{\partial x} - \frac{\partial Bx}{\partial y}\right)$$

where the Bx, By, Bz are the components of the coronal magnetic field extrapolated from the photospheric magnetograms (computed in section 2).

We have computed this parameter for each minute and displayed in figure 3.

What we learn from figure 3 plot: we remark an abrupt increase of the torsion after $20:07$ with a peak at $20:08$ and a graduate decrease next two minutes. Similar scenario repeated with a peak at $20:12$. This α parameter evolution actually indicates the occurrence of two flares, or one double-peak flare, at, respectively $20:08$ and

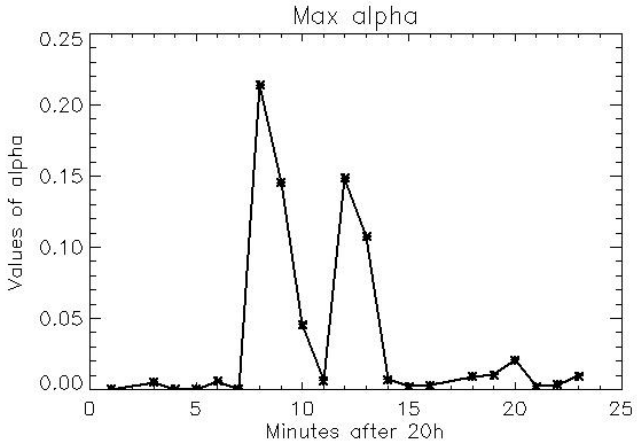

Fig. 3 – The magnetic helicity evolution in AR9845.

$20:12$ o'clock, on 2 March 2002, *i.e.* the C4 and SF flares registered by NOAA. The timing of the SF is slightly different, and we trust more in our estimation since the results of the MHD simulations (next section) indicate the same time.

This result of the torsion computation indicate us the optimal time interval for which we will perform simulations. Using the extrapolated magnetic field, we will analyse in next section the aspect of the initial 3D coronal magnetic field and the results of the numerical experiments, for each minute separately.

5. NUMERICAL SIMULATIONS

As we describe in section 2, the first step of the computations was the preparation of the observational data for the MHD numerical simulations. This preparation consisted in the 3D coronal magnetic field extrapolations starting with magnetograms of the active regions, for each moment, magnetograms similar to that in figure 1. The data sets (Bx, By, Bz) obtained from each magnetogram extrapolation were used as initial input for the simulations, performed with the Alfven code (Weber, 1978) based on SHASTA method (Boris and Book, 1973), for integration of the MHD equations. The code is two-dimensional and we have performed computations in the XOZ plane. Each simulation usually run to produce the evolution of the solar structure for few minutes, until the next magnetogram has to be considered as initial data and new simulations have to be initiated.

The MHD simulations have been performed for one solar radius and with the following values for plasma parameters: $\beta = 0.1$ and the Reynolds number $R_m = 10^2$. The results are displayed in figures 4-11: the 3D coronal magnetic field

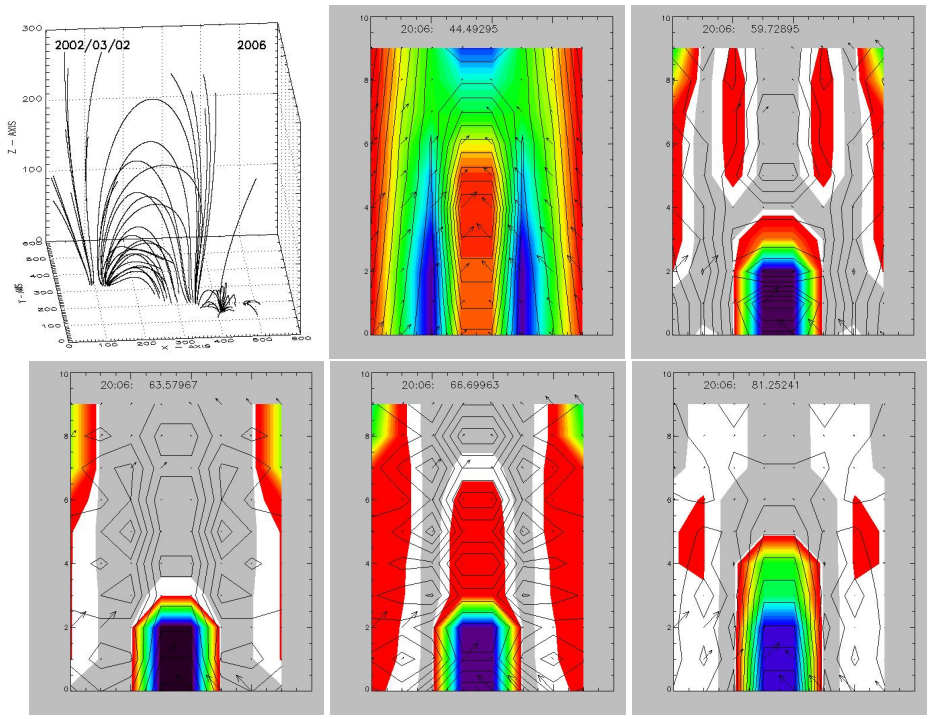

Fig. 4 – The 3D coronal magnetic field extrapolation at 20:06 UT, used as initial magnetic field values and the results of MHD simulations in the ZOX plane.

extrapolation, used as initial value for the MHD simulations, together with the results of the numerical experiments. First of all, must say that a simulation was ended when a stable magnetic structure was obtained, or when numerical instabilities appeared. We comment in the following paragraph the obtained results.

At 20:06 UT as starting time for the simulations, the simulations indicated the formation and evolution of a coronal loop magnetic configuration, where the plasma was partly expelled, but most of it was confined into the closed magnetic field. At 20:07 UT, when the initial coronal field displayed open magnetic field lines too, the magnetic loop stretched until erupted first as a compact flare and later as triggering out its feet too. When the magnetic structure lost a lot of plasma, magnetic reconnections occurred and a new loop formed.

At 20:08 UT, we see a growing coronal loop that breaks in more filamentary structures, erupted and reformed back to erupt again. A cavity structure, with low density material appeared under the loop, as a natural consequence when the material exhausted. Strong velocity field pushed the matter up from below the loop. At 20:09 UT, the initial magnetic magnetic field displays lateral open field lines and a complicated structure suggesting the existence of reconnections in zone. The simulations

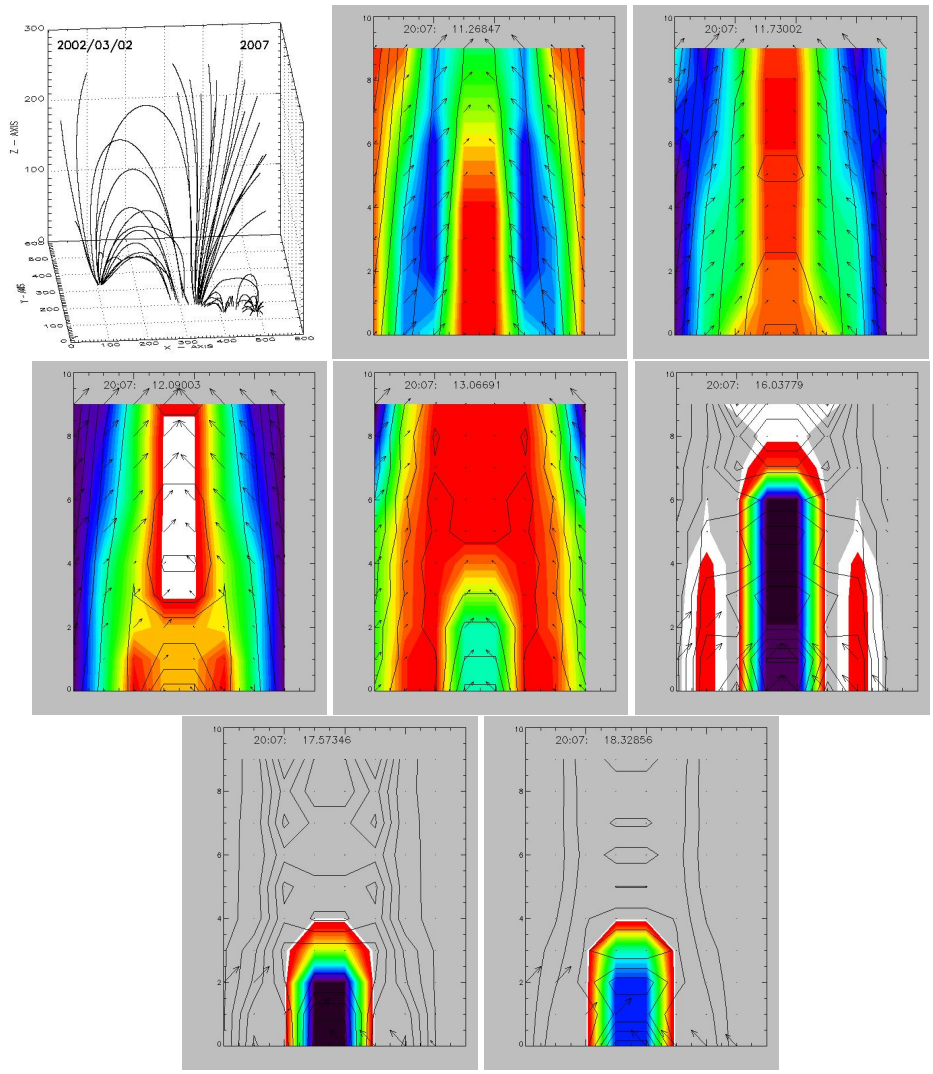

Fig. 5 – The 3D coronal magnetic field extrapolation at 20:07 UT, used as initial magnetic field values and the results of MHD simulations in the ZOX plane.

revealed such reconnections and the opening and closing back of the magnetic field. The central base cavity still exists and the lateral plasma is pushed up continuously. At 20:10 UT, the initial magnetic field displays magnetic loops at different levels with a cavity between them, and a confined magnetic zone at the right side. The simulations gave consecutive loops and cavities rising up in the solar atmosphere, with significative up motions pushing the plasma material. Same scenario repeated at 20:11 UT, when magnetic reconnections produced and the plasma was expelled from

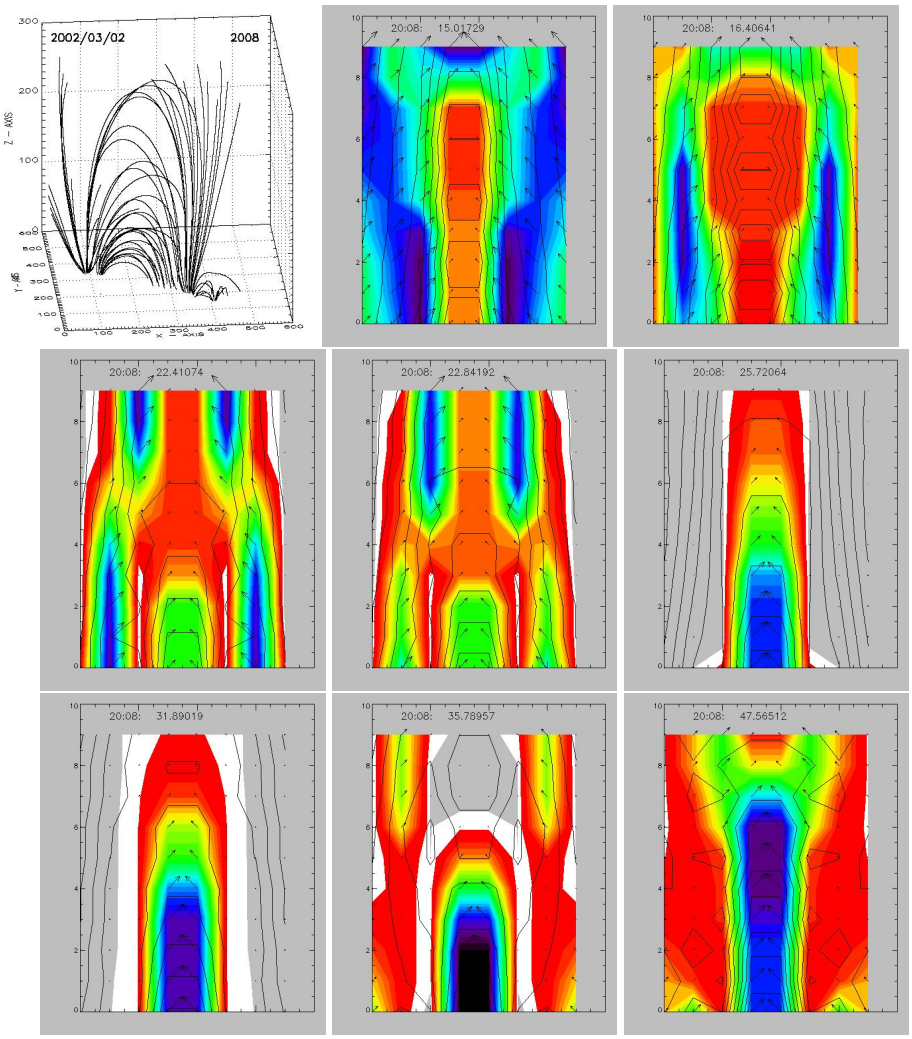

Fig. 6 – The 3D coronal magnetic field extrapolation at 20:08 UT, used as initial magnetic field values and the results of MHD simulations in the ZOX plane.

the grid zone. The initial magnetic configuration had few open magnetic lines on the lateral sides of the loops. At 20:12 UT we obtained a temporary stable structure after 5.52 seconds. It displays loops and lateral open magnetic field lines. The previous scenarios repeated at 20:13 UT, when magnetic loops formed and there were pushed up together with the both sides material. These continuous movements led to magnetic reconnections and central current sheet formation, and finally to changes of the magnetic configurations with permanent release of plasma in the solar atmosphere.

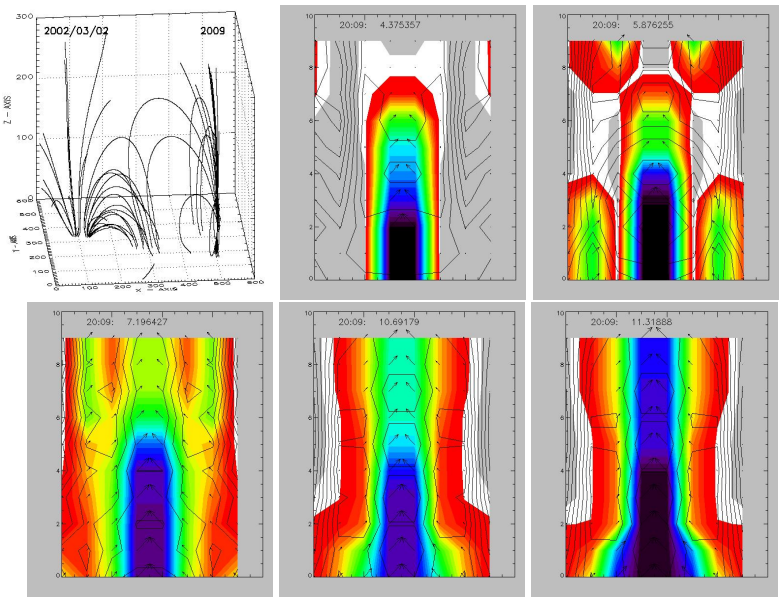

Fig. 7 – The 3D coronal magnetic field extrapolation at 20:09 UT, used as initial magnetic field values and the results of MHD simulations in the ZOX plane.

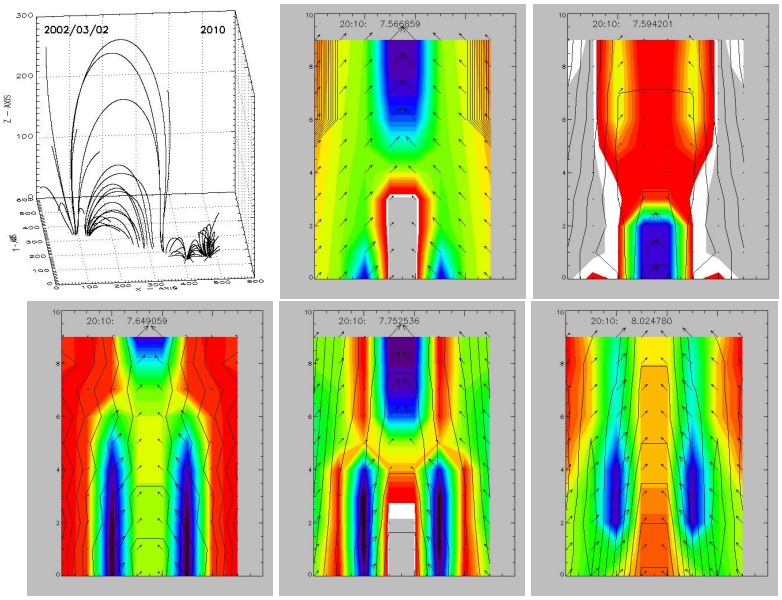

Fig. 8 – The 3D coronal magnetic field extrapolation at 20:10 UT, used as initial magnetic field values and the results of MHD simulations in the ZOX plane.

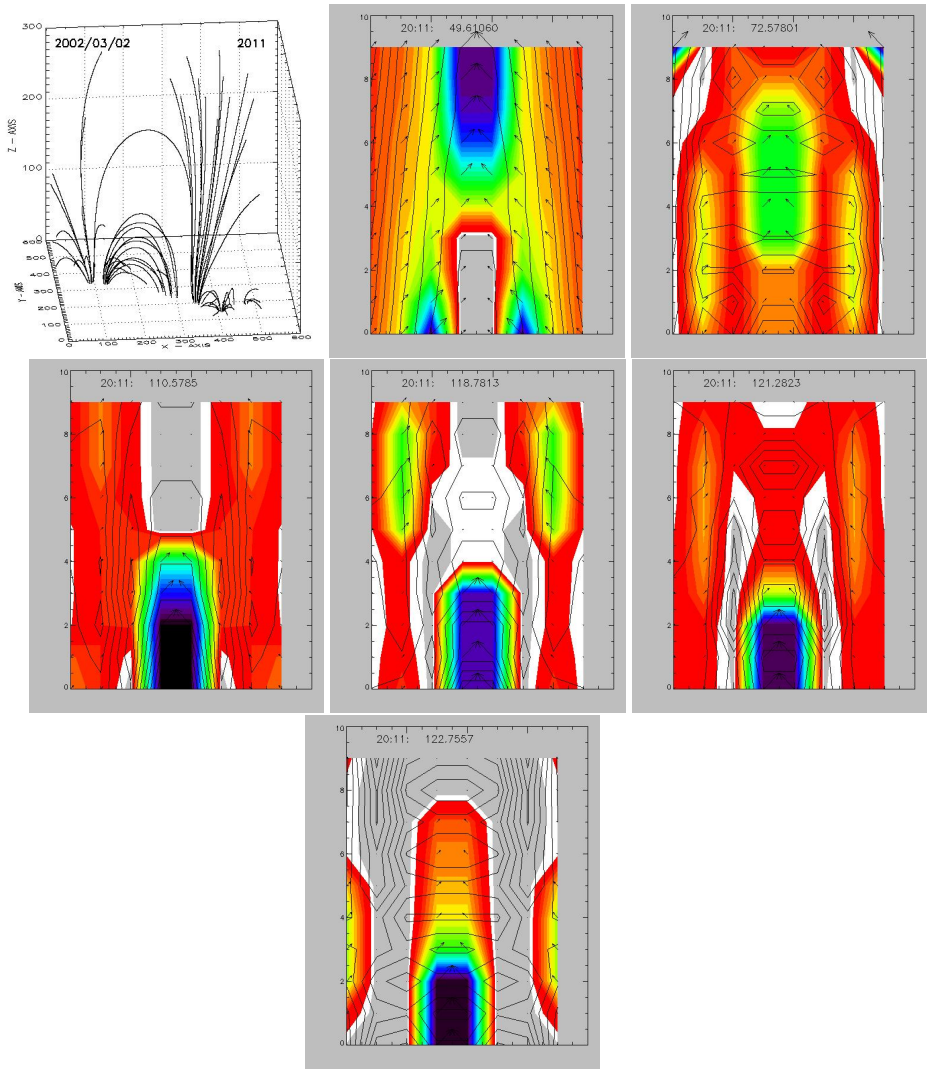

Fig. 9 – The 3D coronal magnetic field extrapolation at 20:11 UT, used as initial magnetic field values and the results of MHD simulations in the ZOX plane.

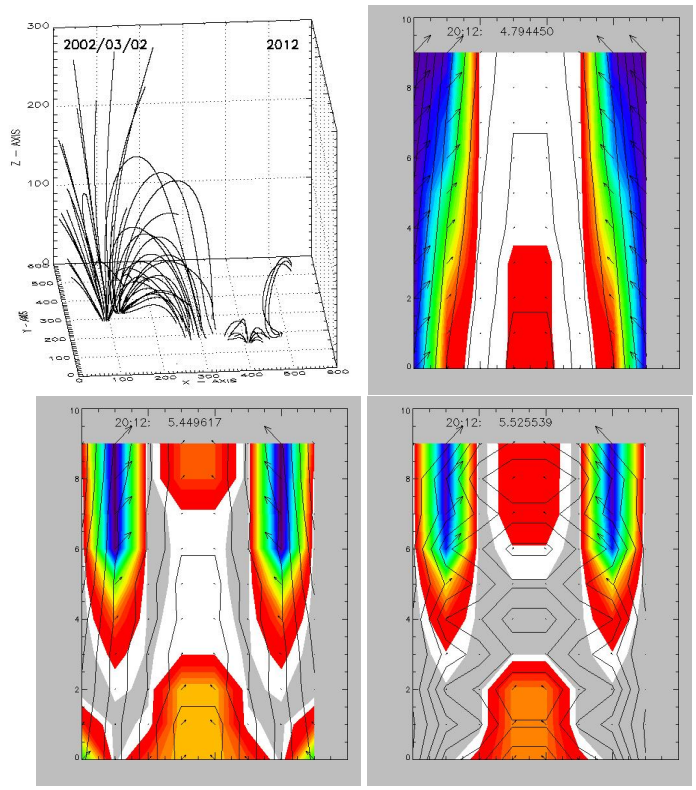

Fig. 10 – The 3D coronal magnetic field extrapolation at 20:12 UT, used as initial magnetic field values and the results of MHD simulations in the ZOX plane.

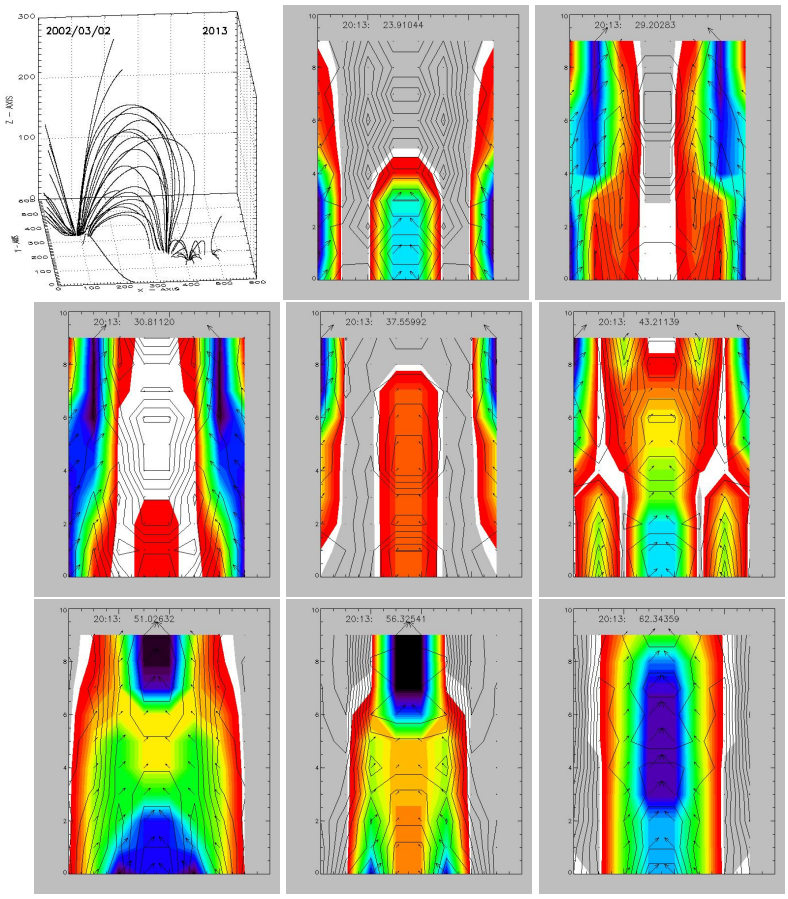

Fig. 11 – The 3D coronal magnetic field extrapolation at 20:13 UT, used as initial magnetic field values and the results of MHD simulations in the ZOX plane.

6. CONCLUSIONS

Our numerical experiments aim was to explore the question of the active regions' numerical modelling starting with real data obtained from solar observations. This topic is very thorny since the non-linear initial magnetic data lead very quickly to numerical instabilities, and numerical unrealistic values at least concerning for the temperatures. The relevant results envisage the magnetic topology evolution, as well as plasma density and velocity field behaviour.

The work implied, at least, two procedures, but we have added also the estimation of the torsion in the active region, inside the time interval when two flares were observed. These estimations straighten the identification of the moments when the explosive events produced. Consequently, the three procedures applied were in this order: (1) the coronal magnetic field extrapolation from the measured photospheric field; (2) the torsion (magnetic helicity) estimation; (3) MHD numerical simulations, starting with the coronal magnetic field as initial values.

The obtained coronal magnetic field, extrapolated from the MDI/SOHO magnetograms, display open and closed magnetic field lines. The open magnetic field lines are indicators of plasma releasing up into the solar corona, and this process happened time to time during all the considered interval. The MHD numerical simulations also revealed the matter expulsion many times, as a consequence of plasma flux emergence and magnetic reconnections. The magnetic field lines torsion estimation revealed two flares occurred at 20:08 UT and 20:12 UT. The MHD numerical simulations revealed the start of the first flare or, at least its' preparation, at 20:07 UT. Plasma insulations, tearing modes and gravitational mode presences are also responsible for the eruptive processes appearance in these simulations. Our results are preliminary ones and they constitute a valuable experience for further works. These types of works are at very beginning stages at the international level.

Acknowledgements. This paper was presented at the International Symposium "The Astronomer Nicolae Donici – 140 years after the birth", Bucharest , 8th September 2014.

REFERENCES

Boris, J.P. and Book, D.L.: 1973, *J.Comp.Phys.* **11**, 38.
Dumitrache C.: 1999, *Romanian Astron. J.* **9**, 139.
Dumitrache, C., Popescu, N.A., Oncica, A.: 2010 *AIP* **1216**, 424.
Fan, Y., Fisher, G. H., DeLuca, E. E.: 1993, *Astrophys. J.* **405**, 390.
Forbes, T.G. and Priest, E.R.: 1982, *Solar Phys.* **81**, 303.
Lee, J.K.: 2002, *Coronal Loop Identification*, Master Thesis, University of Alabama in Huntsville.
Lee, J.K., Gary, G.A., Newman,T.S.: 2003, *Bulletin of the American Astronomical Society* **35**, 809.
Stenflo, J. O.: 1989, *The Astronomy and Astrophysics Review* **1**(1), 3.

Weber, W.J.: 1978, *The dynamics of coronal magnetic structures: a numerical analysis of coronal magnetic field evolution in the presence of large gradients*, PhD Thesis No.408 Utrecht.
Weber, W.J., Boris, J.P. and Gardner, J.H.: 1979, *Computer Physics Communications* **16**, 243.

Received on 15 September 2015